On the domain integral equation method for anisotropic inhomogeneous waveguides

On the Domain Integral Equation Method for Anisotropic Inhomogeneous Waveguides

H. Paul Urbach and Eugène S. A. M. Lepelaars

Abstract—**The domain integral equation method for anisotropic inhomogeneous dielectric waveguides is derived, and the spectral properties of the integral operator are discussed. It is explained why spurious modes do not occur when the Galerkin method is applied to the domain integral equation. Furthermore, the convergence of the method is discussed.**

I. Introduction

ACCURATE methods for the computation of propagation constants and field distributions of guided modes in dielectric waveguides are of great importance for the optimization of optical waveguides. The finite element method (FEM) for the Maxwell equations is widely used in the theoretical study of the complete vector formulation of the physical problem. Reviews of numerical studies of optical dielectric waveguides, in general, and the FEM, in particular, have appeared in [20], [23], and [24]. The fact that the FEM is an exact and general method that can be applied to both inhomogeneous and anisotropic guides explains its popularity. It is less well known that there exists another exact method which is based on a Green's function approach to the Maxwell equations and which is just as general as the FEM. The first publications on this so-called domain integral equation method were probably [1], [2], [19], and [22].

The domain integral equation method has certain advantages over the FEM applied to Maxwell's equations. In the FEM, one has to face the problem of how to incorporate the unbounded region outside the guide. Most authors either employ special large elements in the discretization of the exterior region [14], [15], [17], [21], or they replace this region by a set of integral equations on the physical boundary or on an imaginary boundary [12], [25]. In contrast, the domain integral equation is an equation for the electric field inside the guide only. The exterior region is conveniently incorporated in the kernel of the integral operator.

A second difficulty with applying the FEM to the partial differential equations is the occurrence of spurious solutions [10], [11]. These nonphysical solutions of the discretized systems of equations fail to converge to a solution of Maxwell's equations when the mesh size is decreased. This is caused by the fact that in many numerical schemes, the divergence equation is not satisfied explicitly, although this equation is necessary to guarantee convergence of the approximating solutions. Spurious modes can be prevented by incorporating the divergence equation in some way into the numerical scheme, e.g., by using special basis functions. Unfortunately, such basis functions tend to be complicated. An important advantage of the domain integral equation method is that spurious solutions cannot occur.

The aim of the present paper is to discuss, in more detail, numerical and computational aspects of the domain integral equation method. In contrast with earlier work [2], in which the method of moments with collocation was used, we apply a Galerkin method to solve the integral equation. The reason is that more mathematical results concerning convergence properties, etc., are available for Galerkin methods than for the more general method of moments. We shall assume that all materials are nonmagnetic and lossless. Furthermore, we assume that the exterior of the guide consists of a homogeneous isotropic dielectric. Although the domain integral equation method applies also to the more general case of a guide embedded in a stratified medium [2], [3], and [16], the assumption of a homogeneous cladding is adopted to simplify the kernel of the integral equation.

The propagation constant of the guided mode occurs as a parameter in the kernel of the domain integral operator. The computation of the guided modes amounts to tuning the propagation constant such that one of the eigenvalues of the integral operator becomes equal to -1. We will discuss the convergence of the Galerkin method and explain why spurious modes do not occur. Furthermore, the performance of the method is compared to previous studies for the classical case of a homogeneous isotropic rectangular waveguide. In applying the Galerkin method, we use rectangular elements with piecewise constant base functions. For these elements and base functions, the Galerkin matrix can be computed very efficiently by an analytical technique proposed by Boersma [4]. This technique, which makes the application of fast Fourier transform techniques superfluous, is described in the Appendix.

II. The Domain Integral Formulation

Let (x_1, x_2, x_3) be a Cartesian coordinate system, and let Ω be the cross section of a waveguide which is uniform parallel to the x_3-axis. The cross section Ω may be disconnected, in which case more than one waveguide is present. The boundary of Ω is assumed to be piecewise smooth. Isolated points at

Manuscript received December 2, 1992; revised March 16, 1993.

H. P. Urbach is with Philips Research Laboratory, 5600 JA Eindhoven, The Netherlands.

E. S. A. M. Lepelaarswas with Philips Research Laboratory, 5600 JA Eindhoven, The Netherlands. He is now with the Department of Electrical Engineering, Eindhoven University of Technology, Eindhoven, The Netherlands.

IEEE Log Number 9213730.

which the normal vector is discontinuous are allowed, but cusps are excluded.

All materials are nonmagnetic with magnetic permeability μ_0. The guide is lossless and is, in general, inhomogeneous and anisotropic. The tensor electric permittivity in a point (x_1, x_2) of the guide Ω is given by a positive definite Hermitian tensor of rank 2: $\underline{\underline{\epsilon}}_1(x_1, x_2)$. We will use the convention that symbols indicating matrices and tensors of rank 2 are underlined twice and that vectors are in bold italic type. In electrooptic effects, all elements of the permittivity tensor are real and the tensor is symmetric; but for magnetooptic phenomena, the off-diagonal elements are complex and the tensor is Hermitian [18].

The assumptions concerning the permittivity imply that the tensor $\underline{\underline{\epsilon}}_1(x_1, x_2)$ has in all points (x_1, x_2) of the guide three real positive eigenvalues (counting multiplicity). The numbers $\epsilon_{1,\,max} \geq \epsilon_{1,\,min} > 0$ will denote, respectively, the maximum, taken over all points (x_1, x_2) in the guide, of the largest eigenvalues of the tensors $\underline{\underline{\epsilon}}_1(x_1, x_2)$, and the minimum taken over all (x_1, x_2) in the guide of the smallest eigenvalues of these tensors, i.e.,

$$\epsilon_{1,\,max} = \max_{(x_1,x_2)\in\bar{\Omega}} \max_{\boldsymbol{V}\in\boldsymbol{C}^3\setminus\{0\}} \frac{\underline{\underline{\epsilon}}_1(x_1, x_2)\boldsymbol{V}\cdot\boldsymbol{V}^*}{\boldsymbol{V}\cdot\boldsymbol{V}^*}$$

$$\epsilon_{1,\,min} = \min_{(x_1,x_2)\in\bar{\Omega}} \min_{\boldsymbol{V}\in\boldsymbol{C}^3\setminus\{0\}} \frac{\underline{\underline{\epsilon}}_1(x_1, x_2)\boldsymbol{V}\cdot\boldsymbol{V}^*}{\boldsymbol{V}\cdot\boldsymbol{V}^*} \quad (1)$$

where $\boldsymbol{V}^*$ is the complex conjugate of the vector $\boldsymbol{V}$. The exterior of the guide consists of a lossless homogeneous isotropic dielectric with permittivity $\epsilon_2 > 0$. It is assumed that

$$\min_{\mathbf{V}\in\mathbf{C}^3\setminus\{0\}} \frac{\epsilon_{=1}(x_1, x_2)\mathbf{V}\cdot\mathbf{V}^*}{\mathbf{V}\cdot\mathbf{V}^*} > \epsilon_2, \quad (2)$$

for all points inside the guide except perhaps for the points on the boundary of the guide where equality may hold. Assumption (2) implies that $\varepsilon_{1\max} > \varepsilon_2$ and $\varepsilon_{1\min} > \varepsilon_2$. An inhomogeneous isotropic waveguide with a continuous permittivity profile which is everywhere larger than ε_2 except on the boundary where $\varepsilon_1 = \varepsilon_2$, is an example of a case for which $\varepsilon_{1\min} = \varepsilon_2$.

We define the permittivity tensor field $\underline{\underline{\epsilon}}$: $\boldsymbol{R}^2 \rightarrow \boldsymbol{C}^3 \times \boldsymbol{C}^3$ by

$$\underline{\underline{\epsilon}}(x_1, x_2) = \begin{cases} \underline{\underline{\epsilon}}_1(x_1, x_2) & \text{for } (x_1, x_2) \text{ in } \Omega \\ \epsilon_2\underline{\underline{I}} & \text{for } (x_1, x_2) \text{ outside } \Omega \end{cases} \quad (3)$$

where $\underline{\underline{I}}$ denotes the identity tensor. We will usually write $\underline{\underline{\epsilon}}_2$ instead of $\epsilon_2\underline{\underline{I}}$. We seek time-harmonic solutions of Maxwell's equations of the form

$$\begin{aligned} \mathcal{E}(x_1, x_2, x_3, t) &= \mathrm{Re}\,\{\boldsymbol{E}(x_1, x_2)e^{i(\beta x_3 - \omega t)}\} \\ \mathcal{H}(x_1, x_2, x_3, t) &= \mathrm{Re}\,\{\boldsymbol{H}(x_1, x_2)e^{i(\beta x_3 - \omega t)}\} \end{aligned} \quad (4)$$

for some β. Substitution of (4) into Maxwell's equation yields, after elimination of the magnetic field,

$$\omega^2\mu_0\underline{\underline{\epsilon}}\boldsymbol{E} - \mathrm{curl}_\beta\mathrm{curl}_\beta\boldsymbol{E} = \boldsymbol{0} \quad (5)$$

where curl_β is the curl operator in which $\partial/\partial x_3$ is replaced by multiplication by $i\beta$, i.e.,

$$\mathrm{curl}_\beta\boldsymbol{E} = \begin{pmatrix} \frac{\partial E_3}{\partial x_2} - i\beta E_2 \\ -\frac{\partial E_3}{\partial x_1} + i\beta E_1 \\ \frac{\partial E_2}{\partial x_1} - \frac{\partial E_1}{\partial x_2} \end{pmatrix}. \quad (6)$$

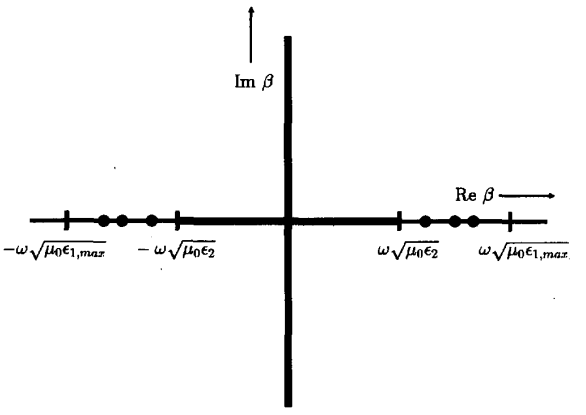

Fig. 1. Solutions for β in the complex plane.

For all real β in the interval $-\omega\sqrt{\epsilon_2\mu_0} \leq \beta \leq \omega\sqrt{\epsilon_2\mu_0}$ and also for all purely imaginary β, there exists nonvanishing solutions of (5) (Fig. 1). The corresponding modes are the radiation and evanescent modes, respectively. Apart from these solutions for β, in general, several real β's are found with

$$\omega^2\mu_0\epsilon_2 < \beta^2 < \omega^2\mu_0\epsilon_{1,\,max} \quad (7)$$

such that to each of these β's there exist a finite number of linear independent nonvanishing solutions $\boldsymbol{E}$ of which the components vanish exponentially with the distance to the guide. These are the guided modes. Because we shall consider guided modes only, we henceforth always assume that β satisfies (7).

In order to derive the domain integral equations, we rewrite (5) as

$$\omega^2\mu_0\underline{\underline{\epsilon}}_2\boldsymbol{E} - \mathrm{curl}_\beta\mathrm{curl}_\beta\boldsymbol{E} = -\omega^2\mu_0(\underline{\underline{\epsilon}} - \underline{\underline{\epsilon}}_2)\boldsymbol{E}. \quad (8)$$

First, we show that for $\beta^2 > \omega^2\mu_0\epsilon_2$, the differential operator on the left-hand side of (8) can be inverted. To compute the inverse, we take the Fourier transform of the equation

$$\omega^2\mu_0\underline{\underline{\epsilon}}_2\boldsymbol{V} - \mathrm{curl}_\beta\mathrm{curl}_\beta\boldsymbol{V} = \boldsymbol{G}. \quad (9)$$

If

$$\mathcal{F}(\boldsymbol{V})(\xi_1, \xi_2) = \int_{-\infty}^{\infty}\int_{-\infty}^{\infty} \exp\left[-2\pi i(\xi_1 x_1 + \xi_2 x_2)\right] \cdot\boldsymbol{V}(x_1, x_2)\,dx_1\,dx_2 \quad (10)$$

then (9) becomes

$$\underline{\underline{\hat{A}}}_\beta^{\epsilon_2}(\xi_1, \xi_2)\mathcal{F}(\boldsymbol{V})(\xi_1, \xi_2) = \mathcal{F}(\boldsymbol{G})(\xi_1, \xi_2) \quad (11)$$

where $\underline{\underline{\hat{A}}}_\beta^{\epsilon_2}(\xi_1, \xi_2)$ denotes the matrix shown in (12), which appears at the bottom of the next page. The derminant of (12) is given by

$$D(\xi_1, \xi_2) = \omega^2\mu_0\epsilon_2\{4\pi^2\xi_1^2 + 4\pi^2\xi_2^2 + \beta^2 - \omega^2\mu_0\epsilon_2\}^2 \quad (13)$$

and since $\beta^2 > \omega^2\mu_0\epsilon_2$, it follows that the matrices $\underline{\underline{\hat{A}}}_\beta^{\epsilon_2}(\xi_1, \xi_2)$ are invertible for all (ξ_1, ξ_2). The inverses of these matrices are given by

$$\underline{\underline{\hat{A}}}_\beta^{\epsilon_2}(\xi_1, \xi_2)^{-1} = \frac{1}{[\omega^2\mu_0\epsilon_2 D(\xi_1, \xi_2)]^{1/2}} \cdot \begin{pmatrix} 4\pi^2\xi_1^2 - \omega^2\epsilon_2\mu_0 & 4\pi^2\xi_1\xi_2 & 2\pi\beta\xi_1 \\ 4\pi^2\xi_1\xi_2 & 4\pi^2\xi_2^2 - \omega^2\epsilon_2\mu_0 & 2\pi\beta\xi_2 \\ 2\pi\beta\xi_1 & 2\pi\beta\xi_2 & \beta^2 - \omega^2\mu_0\epsilon_2 \end{pmatrix}. \quad (14)$$

Hence, (11) can be inverted and, after an inverse Fourier transform, one finds

$$\boldsymbol{V} = \mathcal{F}^{-1} \circ (\underline{\underline{\hat{A}}}_\beta^{\epsilon_2})^{-1} \circ \mathcal{F}(\boldsymbol{G}). \quad (15)$$

By substituting $\boldsymbol{E}$ for $\boldsymbol{V}$ and $-\omega^2\mu_0(\underline{\underline{\epsilon}} - \underline{\underline{\epsilon}}_2)\boldsymbol{E}$ for $\boldsymbol{G}$ in (15), we find that (8) is equivalent to

$$-\boldsymbol{E} = \mathcal{F}^{-1} \circ (\underline{\underline{\hat{A}}}_\beta^{\epsilon_2})^{-1} \circ \mathcal{F}[\omega^2\mu_0(\underline{\underline{\epsilon}} - \underline{\underline{\epsilon}}_2)\boldsymbol{E}]. \quad (16)$$

It will be convenient to symmetrize the operator on the right-hand side of (16). First, we note that it follows from (2) that for all points (x_1, x_2) in the guide, the symmetric tensor $\underline{\underline{\epsilon}}_1(x_1, x_2) - \underline{\underline{\epsilon}}_2$ is nonnegative so that the square roots $(\underline{\underline{\epsilon}}_1(x_1, x_2) - \underline{\underline{\epsilon}}_2)^{1/2}$ are well defined and invertible in Ω. Define the field $\boldsymbol{F}$ by

$$\boldsymbol{F} = (\underline{\underline{\epsilon}} - \underline{\underline{\epsilon}}_2)^{1/2}\boldsymbol{E}. \quad (17)$$

Then $\boldsymbol{F} = 0$ outside of Ω and (16) implies that

$$\boldsymbol{F} + \omega^2\mu_0(\underline{\underline{\epsilon}} - \underline{\underline{\epsilon}}_2)^{1/2}\mathcal{F}^{-1} \circ (\underline{\underline{\hat{A}}}_\beta^{\epsilon_2})^{-1} \circ \mathcal{F}[(\underline{\underline{\epsilon}} - \underline{\underline{\epsilon}}_2)^{1/2}\boldsymbol{F}] = \boldsymbol{0} \quad \text{on } \Omega. \quad (18)$$

It is useful to apply some results from the theory of bounded symmetric operators. We therefore introduce the space $L^2(\Omega)^3$ of all vector fields $\boldsymbol{F}$: $\Omega \to \boldsymbol{C}^3$ with components F_i that are square integrable over the cross section of the guide, i.e.,

$$\int_\Omega\int |F_i(x_1, x_2)|^2\, dx_1\, dx_2 < \infty \quad \text{for } i = 1, 2, 3. \quad (19)$$

The scalar product on $L^2(\Omega)^2$ is given by

$$(\boldsymbol{F}, \boldsymbol{G}) = \int_\Omega\int (F_1G_1^* + F_2G_2^* + F_3G_3^*)\, dx_1\, dx_2. \quad (20)$$

Let the operator $T_\beta^{\underline{\underline{\epsilon}}}$, which acts on fields $\boldsymbol{F}$ in the space $L^2(\Omega)^3$, be defined by

$$T_\beta^{\underline{\underline{\epsilon}}}(\boldsymbol{F}) = \omega^2\mu_0(\underline{\underline{\epsilon}} - \underline{\underline{\epsilon}}_2)^{1/2}\mathcal{F}^{-1} \circ (\underline{\underline{\hat{A}}}_\beta^{\epsilon_2})^{-1} \circ \mathcal{F}[(\underline{\underline{\epsilon}} - \underline{\underline{\epsilon}}_2)^{1/2}\boldsymbol{F}]. \quad (21)$$

Note, that in computing the Fourier transform $\mathcal{F}[(\underline{\underline{\epsilon}} - \underline{\underline{\epsilon}}_2)^{1/2}\boldsymbol{F}]$, the field $\boldsymbol{F}$ on Ω is identified with its extension to the whole plane by putting $\boldsymbol{F} = \boldsymbol{0}$ in the exterior of Ω. It is not difficult to verify that since β is real, $T_\beta^{\underline{\underline{\epsilon}}}$ is a bounded symmetric operator in $L^2(\Omega)^3$, i.e.,

$$(T_\beta^{\underline{\underline{\epsilon}}}(\boldsymbol{F}), \boldsymbol{G}) = (\boldsymbol{F}, T_\beta^{\underline{\underline{\epsilon}}}(\boldsymbol{G})) \quad (22)$$

for all $\boldsymbol{F}$ and $\boldsymbol{G}$ in $L^2(\Omega)^3$. With definition (21), (18) becomes

$$\boldsymbol{F} + T_\beta^{\underline{\underline{\epsilon}}}(\boldsymbol{F}) = \boldsymbol{0} \quad \text{on } \Omega. \quad (23)$$

This is the domain integral equation. The reason for using (23) with (21) as definition of $T_\beta^{\underline{\underline{\epsilon}}}$, instead of the operator on the right-hand side of (16), is that $T_\beta^{\underline{\underline{\epsilon}}}$ is symmetric, i.e., it satisfies (22), whereas the right-hand side of (16) does not.

By computing the Fourier transforms in (21), one can write $\mathcal{F}^{-1} \circ (\underline{\underline{\hat{A}}}_\beta^{\epsilon_2})^{-1} \circ \mathcal{F}$ as a matrix operator with elements that are convolution operators with as kernels certain partial derivatives with respect to x_1 and x_2 of the function $K_0(\sqrt{\beta^2 - \omega^2\mu_0\epsilon_2}(x_1^2 + x_2^2)^{1/2})$, where K_0 is the modified Bessel function of the second kind. These kernels are strongly singular, and the resulting representation of the operator $T_\beta^{\underline{\underline{\epsilon}}}$ is therefore not more convenient than the expression (21) in terms of the Fourier transforms.

The preceding derivation shows that if β is the propagation constant of a guided mode with $\boldsymbol{E}$ as the electric field, then the field $\boldsymbol{F}$ defined on Ω by (17) is an eigenfield of the operator $T_\beta^{\underline{\underline{\epsilon}}}$ with eigenvalue -1. Conversely, if a real β satisfying (7) is such that one of the eigenvalues of the operator $T_\beta^{\underline{\underline{\epsilon}}}$ is equal to -1, then β is a propagation constant of a guided mode. The corresponding electric field can be computed from the eigenfield $\boldsymbol{F}$ by combining (16) and (17)

$$\boldsymbol{E} = -\omega^2\mu_0\mathcal{F}^{-1} \circ (\underline{\underline{\hat{A}}}_\beta^{\epsilon_2})^{-1} \circ \mathcal{F}[(\underline{\underline{\epsilon}} - \underline{\underline{\epsilon}}_2)^{1/2}\boldsymbol{F}]. \quad (24)$$

When one is only interested in the electric field inside the guide, it suffices to invert (17).

We remark that the domain integral formulation cannot be applied to radiation and evanescent modes. The derivation of (23) does not apply for these modes because when $\beta^2 \leq \omega^2\mu_0\epsilon_2$, (9) cannot be inverted, as follows immediately from the vanishing of the determinant (13) for $\xi_1^2 + \xi_2^2 = (\omega^2\mu_0\epsilon_2 - \beta^2)/4\pi^2$.

In order to apply the domain integral equation to the problem of the determination of guided modes, it is essential to analyze the spectrum of $T_\beta^{\underline{\underline{\epsilon}}}$. Because $T_\beta^{\underline{\underline{\epsilon}}}$ is a bounded symmetric operator, its spectrum is a bounded subset of the real axis [9]. It can be shown [26] that all λ in the spectrum satisfy

$$-\frac{\omega^2\mu_0\epsilon_{1,\,max} - \omega^2\mu_0\epsilon_2}{\beta^2 - \omega^2\mu_0\epsilon_2} < \lambda \leq \frac{\epsilon_{1,\,max} - \epsilon_2}{\epsilon_2}. \quad (25)$$

Furthermore, the negative part of the spectrum consists of a countable set of eigenvalues λ_n, $n = 1, 2, \cdots$, which when

---

$$\underline{\underline{\hat{A}}}_\beta^{\epsilon_2}(\xi_1, \xi_2) = \begin{pmatrix} \omega^2\mu_0\epsilon_2 - \beta^2 - 4\pi^2\xi_2^2 & 4\pi^2\xi_1\xi_2 & 2\pi\beta\xi_1 \\ 4\pi^2\xi_1\xi_2 & \omega^2\mu_0\epsilon_2 - \beta^2 - 4\pi^2\xi_1^2 & 2\pi\beta\xi_2 \\ 2\pi\beta\xi_1 & 2\pi\beta\xi_2 & \omega^2\mu_0\epsilon_2 - 4\pi^2(\xi_1^2 + \xi_2^2) \end{pmatrix}. \quad (12)$$

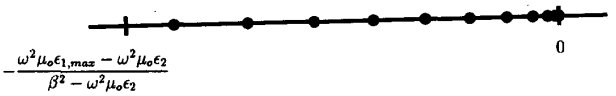

Fig. 2. Impression of the negative part of the spectrum of the domain integral operator $T^{\underline{\epsilon}}_{\beta}$.

ordered and counting multiplicities, satisfy (see Fig. 2)

$$-\frac{\omega^2\mu_0\epsilon_{1,\,max}-\omega^2\mu_0\epsilon_2}{\beta^2-\omega^2\mu_0\epsilon_2}<\lambda_1\le\lambda_2\le\cdots\le\lambda_n\le\cdots<0 \tag{26}$$

and

$$\lim_{n\to\infty}\lambda_n=0. \tag{27}$$

Every λ_n is equal to at most a finite number of the other eigenvalues. The degeneracy of the eigenvalues depends on the symmetry properties of the guide and of the permittivity.

The determination of the positive part of the spectrum $T^{\underline{\epsilon}}_{\beta}$ is difficult. It may be (partly) continuous spectrum. For the computation of guided modes, however, only the negative part of the spectrum is of interest.

III. The Determination of the Guided Modes

Let β satisfy (7). Let $\lambda_1(\beta)$ be the smallest eigenvalue of the operator $T^{\underline{\epsilon}}_{\beta}$. Because $T^{\underline{\epsilon}}_{\beta}$ is a bounded symmetric operator, $\lambda_1(\beta)$ has the following characterization [27], [6]:

$$\lambda_1(\beta)=\min_{\boldsymbol{F}\in L^2(\Omega)^3\setminus\{0\}}R(\boldsymbol{F}) \tag{28}$$

where R is the Rayleigh quotient

$$R(\boldsymbol{F})=\frac{(T^{\underline{\epsilon}}_{\beta}(\boldsymbol{F}),\,\boldsymbol{F})}{(\boldsymbol{F},\,\boldsymbol{F})},\qquad \boldsymbol{F}\neq 0. \tag{29}$$

Under the hypothesis (2) for the electric permittivity, it can be proved [26] that for waveguides of arbitrary cross sections, one has

$$\lim_{\beta\downarrow\omega\sqrt{\epsilon_2\mu_0}}\lambda_1(\beta)=-\infty \tag{30}$$

$$\lim_{\beta\uparrow\omega\sqrt{\epsilon_{1,\,max}\mu_0}}\lambda_1(\beta)>-1. \tag{31}$$

This is illustrated in Fig. 3, where the numerically computed smallest five eigenvalues are drawn as function of β for a particular waveguide. Because the operator $T^{\underline{\epsilon}}_{\beta}$ depends continuously on β, so do the eigenvalues. We thus conclude from (30) and (31) that there exists at least one β with $\omega^2\mu_0\epsilon_2<\beta^2<\omega^2\mu_0\epsilon_{1,\,max}$ such that $\lambda_1(\beta)=-1$.

One can also consider the other eigenvalues $\lambda_2(\beta)\le\lambda_3(\beta)\le\cdots$ (repeated according to their multiplicites). The mini–max principle [6] implies the following characterization of these eigenvalues:

$$\lambda_n(\beta)=\min_{W_n}\max_{\boldsymbol{F}\in W_n\setminus\{0\}}R(\boldsymbol{F}) \tag{32}$$

where the minimum is taken over all n-dimensional subspaces of the space $L^2(\Omega)^3$. It can be shown that λ_2 also has the properties (30) and (31). Hence, $\lambda_2(\beta)$ also intersects the line

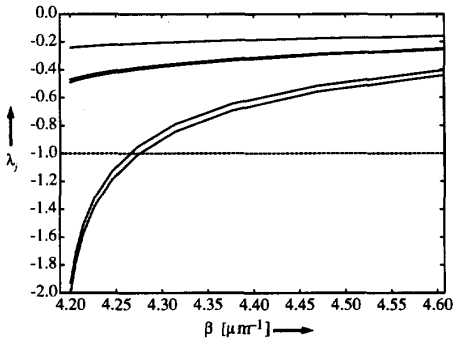

Fig. 3. Plot of the eigenvalues $\lambda_j(\beta)$, $j=1,2,3,4,5$, for a waveguide with rectangular cross section with edges of 2 μm × 1 μm. The guide is homogeneous and isotropic with refractive index 1.1, and the exterior region has refractive index 1.0. The wavelength in vacuo is 1.5 μm. The mesh consisted of 20 × 10 rectangles.

$\lambda=-1$ at least once, with a propagation constant smaller than or equal to the one corresponding to the smallest eigenvalue. We thus conclude that for all waveguides of arbitrary cross section with permittivity $\underline{\epsilon}_1$ satisfying (2), there are at least two guided modes. In this statement, we count the number of linear independent electromagnetic fields that are guided, and not the number of propagation constants as most authors do. In the case of symmetry, some eigenvalues may coincide, and then there are linearly independent guided mode fields with identical propagation constants. This happens, for instance, with the smallest two eigenvalues for the circle and the square waveguide (see Fig. 5). However, in general, linear independent fields have different propagation constants, hence, in general, one has at least two propagation constants.

In contrast to the smallest two eigenvalues, the larger eigenvalues do not satisfy (30). For $n\ge 3$, the limits

$$\lim_{\beta\downarrow\omega\sqrt{\mu_0\epsilon_2}}\lambda_n(\beta) \tag{33}$$

are finite negative numbers (see Fig. 3). For given cross section Ω, this limit is smaller than -1 only when $\omega^2\mu_0(\epsilon_{1,\,max}-\epsilon_2)$ is sufficiently large. If this is not the case, then one cannot expect the function $\lambda_n(\beta)$ to vanish for a certain β. In general, for a given cross section and given permittivities, there exists an integer $m\ge 3$ such that for all $n\ge m$, the $\lambda_n(\beta)$ do not have a zero. The modes corresponding to these eigenvalues are not guided.

Although there is numerical evidence that the λ_n are monotonically increasing functions of $\beta>0$, this has not been demonstrated rigorously. If it were true, every eigenvalue λ_n of $T^{\underline{\epsilon}}_{\beta}$ would correspond to at most one guided mode, and the criterion that the limit in (33) has to be smaller than -1 would not only be sufficient but also necessary for the mode corresponding to λ_n to be guided.

IV. The Eigenvalue Problem for $T^{\underline{\epsilon}}_{\beta}$

For a given β with $\omega^2\mu_0\epsilon_2<\beta^2<\omega^2\mu_0\epsilon_{1,\,max}$, we consider the numerical computation of the nth eigenvalue λ_n and the corresponding eigenfield $\boldsymbol{F}$ of the operator $T^{\underline{\epsilon}}_{\beta}$

$$\lambda_n\boldsymbol{F}-T^{\underline{\epsilon}}_{\beta}(\boldsymbol{F})=\boldsymbol{0}. \tag{34}$$

Equation (34) is equivalent to the following variational problem:

$$\lambda_n(\boldsymbol{F}, \boldsymbol{G}) - (T_\beta^\epsilon(\boldsymbol{F}), \boldsymbol{G}) = 0 \qquad \text{for all } \boldsymbol{G} \in L^2(\Omega)^3 \quad (35)$$

where $(\cdot, \cdot)$ is, as before, the scalar product on $L^2(\Omega)^3$. The eigenvalue problem will be solved by applying the Galerkin method to this variational problem.

For $h > 0$, consider a grid with maximum mesh size h which discretizes Ω, and let V_h be a finite-dimensional space of functions on this grid. In the following, the subscript h is assumed to be in a countable set of positive numbers which accumulate only in 0. Furthermore, it is assumed that the spaces V_h are such that for every function f in $L^2(\Omega)$ and for every δ, there exists for all sufficiently small h a function in V_h which approximates f with error smaller than δ. The spaces $V_h^3 = V_h \times V_h \times V_h$ are the finite-dimensional subspaces of $L^2(\Omega)^3$ in which the approximate solutions of (34) are computed. The approximate variational problem is

Find real λ_{nh} and $\boldsymbol{F}_h$ in V_h^3, with $\boldsymbol{F}_h \neq \boldsymbol{0}$, such that

$$\lambda_{nh}(\boldsymbol{F}_h, \boldsymbol{G}) - (T_\beta^\epsilon(\boldsymbol{F}_h), \boldsymbol{G}) = 0 \qquad \text{for all } \boldsymbol{G} \in V_h^3. \quad (36)$$

It is a distinctive property of the Galerkin method, compared to the more general methods of moments, that the weight functions $\boldsymbol{G}$ are chosen from the same space as that in which the solution is approximated.

Note that the bilinear form $(\boldsymbol{F}_h, \boldsymbol{G})$ on the left-hand side of (36), in general, does not lead to a diagonal matrix, let alone a multiple of the identity matrix; although it is, in general, diagonal dominant. Hence, the approximate problem is usually a *generalized* eigenvalue problem. Nevertheless, the mini–max principle also applies to the approximate problem, and hence the nth generalized eigenvalue (counting multiplicites) satisfies

$$\lambda_{nh} = \min_{W_{nh}} \max_{\boldsymbol{G} \in W_{nh} \setminus \{0\}} R(\boldsymbol{G}) \quad (37)$$

where the minimum is taken over all n-dimensional subspaces of V_h^3. By comparing (32) and (37), it follows immediately that

$$\lambda_n \leq \lambda_{nh} \quad (38)$$

for every $h > 0$. Hence, the eigenvalues are always approximated from above. Furthermore, it is evident that

$$\lim_{h \to 0} \lambda_{nh} = \lambda_n. \quad (39)$$

Using this result and a specific property of the bilinear form $(T_\beta^\epsilon(\boldsymbol{F}_h), \boldsymbol{G})$, it can be deduced [26] that the solutions $\boldsymbol{F}_h$ of the finite-dimensional minimization problems (37) converge to a solution $\boldsymbol{F}$ of the continuous solution: $\lim_{h \to 0} \|\boldsymbol{F}_h - \boldsymbol{F}\| = 0$. Since the latter is the physical solution, it follows that spurious solutions cannot occur.

The error made in approximating the eigenvalues can be expressed in terms of the error made in approximating the fields. Using (35), (36), and the symmetry of T_β^ϵ, we find

$$\begin{aligned}
&(T_\beta^\epsilon(\boldsymbol{F} - \boldsymbol{F}_h), \boldsymbol{F} - \boldsymbol{F}_h) \\
&= (T_\beta^\epsilon(\boldsymbol{F}), \boldsymbol{F} - \boldsymbol{F}_h) - (\boldsymbol{F}_h, T_\beta^\epsilon(\boldsymbol{F})) + (T_\beta^\epsilon(\boldsymbol{F}_h), \boldsymbol{F}_h) \\
&= \lambda_n(\boldsymbol{F}, \boldsymbol{F} - \boldsymbol{F}_h) - \lambda_n(\boldsymbol{F}_h, \boldsymbol{F}) + \lambda_{nh}(\boldsymbol{F}_h, \boldsymbol{F}_h) \\
&= \lambda_n(\boldsymbol{F} - \boldsymbol{F}_h, \boldsymbol{F} - \boldsymbol{F}_h) + (\lambda_{nh} - \lambda_n)(\boldsymbol{F}_h, \boldsymbol{F}_h). \quad (40)
\end{aligned}$$

The continuity of T_β^ϵ implies that for some constant $C_\beta > 0$, depending on β but not on $\boldsymbol{G}$, the following inequality holds:

$$\left|(T_\beta^\epsilon(\boldsymbol{G}), \boldsymbol{G})\right| \leq C_\beta \|\boldsymbol{G}\|^2 \quad (41)$$

where $\|\cdot\|$ is the norm on $L^2(\Omega)^3$. If we assume that the $\boldsymbol{F}_h$ are all normalized such that $\|\boldsymbol{F}_h\| = 1$, then we infer from (40) and (41) that

$$\lambda_{nh} - \lambda_n \leq (C_\beta + |\lambda_n|)\|\boldsymbol{F} - \boldsymbol{F}_h\|^2. \quad (42)$$

Hence, the error in computing the approximated eigenvalues is bounded from above by the square of the error made in computing the fields. Because the approximate propagation constants β_h are determined by solving iteratively the equations

$$\lambda_{nh}(\beta) = 0 \quad (43)$$

for fixed n, it is clear that when $d\lambda_n/d\beta \neq 0$ in a neighborhood of the exact propagation constant β, the error in the approximate propagation constants is also bounded by the square of the error made in the computation of the fields $\boldsymbol{F}$.

Using the smoothness of the field $\boldsymbol{F}$ and results from interpolation theory [5], the error $\|\boldsymbol{F} - \boldsymbol{F}_h\|$ can, in general, be estimated by a number that is proportional to a power of the mesh size h. This power is referred to as the order of convergence. It depends on the choice for the spaces V_h, on the smoothness of the electric permittivity and on the smoothness of the guide. For the case of rectangular elements with piecewise constant base functions, the interpolation error for a rectangular waveguide was found to be $\mathcal{O}(h)$; hence, the error in approximating the eigenvalues λ_n and the corresponding propagation constants is $\mathcal{O}(h^2)$ in this case.

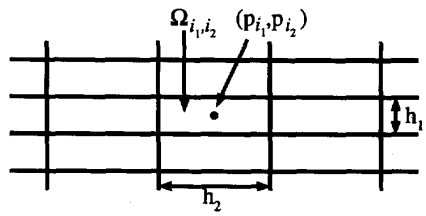

Fig. 4. Rectangular element with nodal point.

V. Numerical Implementation and Results

We consider a grid of rectangular elements whose edges are parallel to the x_1- and x_2-axis (Fig. 4). Although the analysis can be generalized to the case of elements with different sizes, we assume for simplicity's sake that all elements have equal size, with h_1 and h_2 being the lengths of the edges parallel to the x_1- and x_2-axis, respectively. Let $\Omega_{i_1 i_2}$ be the element of

which the midpoint has coordinates $x_1 = p_{i_1}$, $x_2 = p_{i_2}$. The basis functions spanning the space V_h with $h = \max(h_1, h_2)$ are defined by

$$1_{\Omega_{i_1 i_2}}(x_1, x_2) = \begin{cases} 1 & \text{if } (x_1, x_2) \text{ is in } \Omega_{i_1 i_2} \\ 0 & \text{otherwise.} \end{cases} \quad (44)$$

Hence, the space $V_h^3 = V_h \times V_h \times V_h$ has as its basis the fields

$$\boldsymbol{G}_{i_1 i_2 k} = 1_{\Omega_{i_1 i_2}} \boldsymbol{e}_k \quad (45)$$

for $k = 1, 2, 3$, where $\boldsymbol{e}_1 = (1, 0, 0)^T$, $\boldsymbol{e}_2 = (0, 1, 0)^T$, and $\boldsymbol{e}_3 = (0, 0, 1)^T$. For the sake of brevity, we define the triple index $\nu = (i_1, i_2, k)$ and write $\boldsymbol{G}_\nu$ instead of $\boldsymbol{G}_{i_1 i_2 k}$. Since the $\boldsymbol{G}_\nu$ form a basis for V_h^3, the solution $\boldsymbol{F}_h$ of the approximate problem (36) can be written as

$$\boldsymbol{F}_h = \sum_\nu u_\nu \boldsymbol{G}_\nu \quad (46)$$

for some complex numbers u_ν. Hence, (36) is equivalent to

$$\sum_\nu \{\lambda_{nh}(\boldsymbol{G}_\nu, \boldsymbol{G}_\mu) - (T_\beta^{\underline{\underline{\epsilon}}}(\boldsymbol{G}_\nu), \boldsymbol{G}_\mu)\} u_\nu = 0 \quad (47)$$

for all μ. Let $\nu = (i_1, i_2, k)$ and $\mu = (j_1, j_2, l)$; then

$$\begin{aligned}(\boldsymbol{G}_\nu, \boldsymbol{G}_\mu) &= \int\int_{\Omega_{i_1 i_2} \cap \Omega_{j_1 j_2}} dx_1\, dx_2\, \boldsymbol{e}_k \cdot \boldsymbol{e}_l \\ &= h_1 h_2 \delta_{i_1, j_1} \delta_{i_2, j_2} \delta_{kl} = h_1 h_2 \delta_{\nu\mu} \end{aligned} \quad (48)$$

where δ_{ab} is Kronecker's symbol, i.e., $\delta_{ab} = 1$ if $a = b$ and $= 0$ otherwise. Hence, the first matrix on the left-hand side of (47) is proportional to the identity matrix. Using (19) and Parseval's identity, we find for the second matrix

$$(T_\beta^{\underline{\underline{\epsilon}}}(\boldsymbol{G}_\nu), \boldsymbol{G}_\mu) = \omega^2 \mu_0 ((\hat{\underline{\underline{A}}}_\beta^{\underline{\underline{\epsilon}}_2})^{-1} \circ \mathcal{F}[(\underline{\underline{\epsilon}} - \underline{\underline{\epsilon}}_2)^{1/2} \boldsymbol{G}_\nu], \mathcal{F}[(\underline{\underline{\epsilon}} - \underline{\underline{\epsilon}}_2)^{1/2} \boldsymbol{G}_\mu]). \quad (49)$$

In order to compute these scalar products, the matrix-valued function $(\underline{\underline{\epsilon}} - \underline{\underline{\epsilon}}_2)^{1/2}$ is interpolated using the piecewise-constant basis functions

$$(\underline{\underline{\epsilon}} - \underline{\underline{\epsilon}}_2)^{1/2} \sim \sum_{i_1, i_2} [\underline{\underline{\epsilon}}(p_{i_1}, p_{i_2}) - \underline{\underline{\epsilon}}_2]^{1/2} 1_{\Omega_{i_1 i_2}}. \quad (50)$$

By substituting this approximation into (49), using the formula

$$\mathcal{F}(1_{\Omega_{i_1 i_2}})(\xi_1, \xi_2) = \exp(-2\pi i \xi_1 p_{i_1}) \frac{\sin(\pi \xi_1 h_1)}{\pi \xi_1} \cdot \exp(-2\pi i \xi_2 p_{i_2}) \frac{\sin(\pi \xi_2 h_2)}{\pi \xi_2} \quad (51)$$

and (14), one finds for $\nu = (i_1, i_2, k)$ and $\mu = (j_1, j_2, l)$, that the number

$$((\hat{\underline{\underline{A}}}_\beta^{\underline{\underline{\epsilon}}_2})^{-1} \circ \mathcal{F}[(\underline{\underline{\epsilon}} - \underline{\underline{\epsilon}}_2)^{1/2} \boldsymbol{G}_\nu], \mathcal{F}[(\underline{\underline{\epsilon}} - \underline{\underline{\epsilon}}_2)^{1/2} \boldsymbol{G}_\mu]) \quad (52)$$

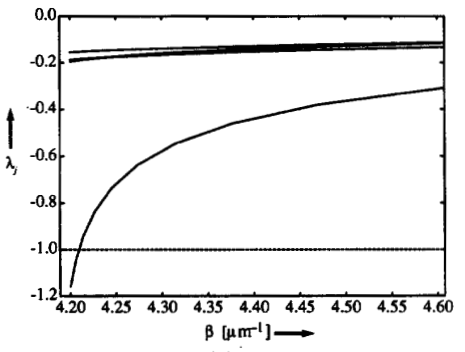

Fig. 5. Plot of the eigenvalues $\lambda_j(\beta)$, $j = 1, 2, 3, 4, 5$, for a waveguide with square cross section with edges of 1 μm. The guide is homogeneous and isotropic with refractive index 1.1, and the exterior region has refractive index 1.0. The wavelength in vacuo is 1.5 μm. The mesh consisted of 10×10 rectangles. Due to the symmetry, the smallest two eigenvalues coincide.

is given by the element (k, l) of the $(3, 3)$ matrix that results after computing the matrix product

$$[\underline{\underline{\epsilon}}(p_{j_1}, p_{j_2}) - \underline{\underline{\epsilon}}_2]^{1/2} \underline{\underline{S}}_\beta(p_{j_1} - p_{i_1}, p_{j_2} - p_{i_2}) \cdot [\underline{\underline{\epsilon}}(p_{i_1}, p_{i_2}) - \underline{\underline{\epsilon}}_2]^{1/2} \quad (53)$$

where for given v_1, v_2, the $(3, 3)$-matrix $\underline{\underline{S}}_\beta(v_1, v_2)$ is defined by (54), which is shown at the bottom of this page where

$$\begin{aligned} I(v_1, v_2, m_1, m_2) &= \int_{-\infty}^{\infty}\int_{-\infty}^{\infty} \frac{(2\pi\xi_1)^{m_1}(2\pi\xi_2)^{m_2}}{(2\pi\xi_1)^2 + (2\pi\xi_2)^2 + \beta^2 - \omega^2\mu_0\epsilon_2} \\ &\quad \cdot \exp(2\pi i \xi_1 v_1 + 2\pi i \xi_2 v_2) \left[\frac{\sin(\pi\xi_1 h_1)}{\pi\xi_1}\right]^2 \\ &\quad \cdot \left[\frac{\sin(\pi\xi_2 h_2)}{\pi\xi_2}\right]^2 d\xi_1\, d\xi_2. \end{aligned} \quad (55)$$

The arguments (v_1, v_2) in (55) have been omitted from (54) for the sake of brevity. The integrals (55) can be evaluated very efficiently using the expressions listed in the Appendix.

By substituting the results (48), (49), (53) into (47), one gets, after dividing by $h_1 h_2$, a matrix eigenvalue problem

$$(\lambda_{nh} I - \tilde{\underline{\underline{S}}}_\beta)\boldsymbol{u} = \boldsymbol{0} \quad (56)$$

where I is the identity, $\tilde{\underline{\underline{S}}}_\beta$ is the matrix obtained by multiplying the right-hand side of (53) by $\omega^2\mu_0/h_1h_2$, and $\boldsymbol{u}$ is the vector with components u_ν. The eigenvalues and eigenvectors of the Hermitian matrix $\tilde{\underline{\underline{S}}}_\beta$ were computed by a BLAS (Basic Linear Algebra Subroutine) routine, which uses Householder transformations to convert $\tilde{\underline{\underline{S}}}_\beta$ into a real tridiagonal symmetric matrix, followed by a QR iteration.

Fig. 5 shows a plot of the smallest 5 eigenvalues as functions of β for a homogeneous isotropic square waveguide with edges

$$\frac{1}{\omega^2\mu_0\epsilon_2} \begin{pmatrix} I(2,0) - \omega^2\mu_0\epsilon_2 I(0,0) & I(1,1) & \beta I(1,0) \\ I(1,1) & I(0,2) - \omega^2\mu_0\epsilon_2 I(0,0) & \beta I(0,1) \\ \beta I(1,0) & \beta I(0,1) & (\beta^2 - \omega^2\mu_0\epsilon_2) I(0,0) \end{pmatrix} \quad (54)$$

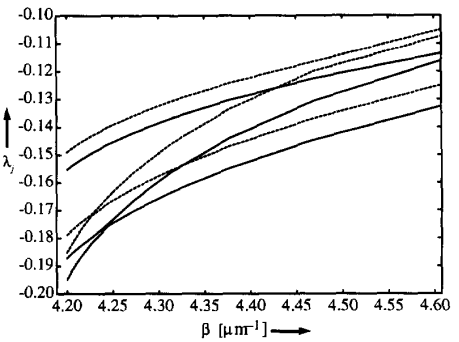

Fig. 6. Comparison of the third, fourth, and fifth eigenvalues as computed using a 10×10 mesh (continuous curves) and a 5×5 mesh (dashed curves). Physical parameters are as in Fig. 5.

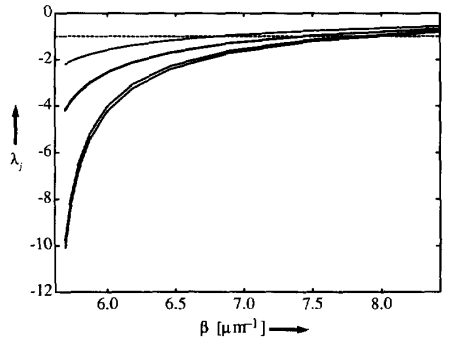

Fig. 7. The smallest five eigenvalues as functions of β for a rectangular waveguide of 2 μm $\times$ 1 μm and refractive index 1.5. The exterior region has refractive index 1.0, the wavelength in vacuo is 1.118 μm. A 5×10 mesh was used. The third and fourth eigenvalues are almost identical and overlap in the figure.

TABLE I
CPU TIMES AND MEMORY REQUIREMENTS FOR SOLVING ONE EIGENVALUE PROBLEM ON SEVERAL MESHES. THE DATA ARE ALMOST THE SAME FOR THE WAVEGUIDES OF FIGS. 3, 5, AND 7

$N_1 \times N_2$	CPU (s)	Memory (Mb)
25	0.1	0.172
100	3	0.687
200	23	2.75
400	175	10.99
1800	20197	222.47

TABLE II
ITERATION TO COMPUTE β CORRESPONDING TO EIGENVALUE $\lambda_1(\beta)$. THE FIRST COLUMN BELOW "CPU" GIVES THE TIME REQUIRED TO BUILD THE MATRIX, THE SECOND COLUMN IS THE TIME NEEDED FOR THE EIGENVALUE CALCULATION. THE DATA CORRESPOND TO THE RECTANGULAR GUIDE OF 2 μm $\times$ 1 μm WITH A 10×15 MESH, WITH REFRACTIVE INDEX $n_1 = 1.1$ AND WITH WAVELENGTH 1 μm

Iteration	β (μm^{-1})	$\lambda_1(\beta)$	CPU (s)
1	6.5973445725	−0.9456377202	0.354 8.292
2	6.4402649399	−1.4175146593	0.353 8.284
3	6.5188047562	−1.1275070159	0.355 8.284
4	6.5684374348	−1.0044327522	0.354 8.244
5	6.5704647705	−1.0000425328	0.350 8.273
6	6.5704845030	−1.0000000137	0.353 8.271
7	6.5704845095	−0.9999999997	0.349 8.292

TABLE III
CONVERGENCE OF PROPAGATION CONSTANTS FOR AN INCREASING NUMBER OF ELEMENTS ON A RECTANGULAR GRID, WITH THE NUMBER OF ELEMENTS GIVEN BY $2N_2 \times N_2$. THE GUIDE IS 2 μm $\times$ 1 μm, $n_1 = 1.5$, AND THE WAVELENGTH IS 1.118 μm

N_2	β_1 (μm^{-1})	β_2 (μm^{-1})	β_3 (μm^{-1})
5	7.906037	7.770163	7.416022
10	7.943407	7.838187	7.514330
15	7.950961	7.852170	7.534289

of 1 μm and with refractive index $n_1 = 1.1$. In this and all other examples, the refractive index of the exterior region is 1. The wavelength in vacuo is 1.5 μm in Fig. 5. The number of rectangles used in the calculations was 10×10. As a consequence of the symmetry, the smallest two eigenvalues coincide. There are thus two linearly independent modes corresponding to the largest propagation constant. The guided modes corresponding to the larger eigenvalues λ_3, λ_4, λ_5 are not guided. In Fig. 6, the graphs of these eigenvalues for the 10×10 grid are compared to the results on a 5×5 grid. In agreement with the mini–max principle, finer meshes yield smaller eigenvalues. In Fig. 7, the smallest 5 eigenvalues are shown for a rectangular guide of dimensions 2 μm $\times$ 1 μm with refractive index $n_1 = 1.5$. The wavelength in vacuo is 1.118 μm. Due to the higher optical contrast and higher frequency, all 5 eigenvalues intersect the line $\lambda = -1$ for a certain β, and hence correspond to guided modes. The computations were performed on a 10×5 mesh.

The CPU time needed for the computation of a particular guided mode is determined by the time needed for solving an eigenvalue problem for given β. In Table I, CPU times and memory requirements for solving an eigenvalue problem typical for the waveguides mentioned above are listed for several rectangular grids. The computations were carried out on an IBM 9121 mainframe with vector facilities. CPU times are strongly machine-dependent, of course. Due to the efficient computation of the integrals (55), explained in the Appendix, only 5% of the CPU was needed for building the matrix, the rest was used for computing the eigenvalue. It should be mentioned that for the storage, use is made of the symmetry of the matrices; but the symmetry of the fields with respect to the x_1- and x_2-axis was not exploited.

To solve the equation $\lambda_n(\beta) = -1$, the eigenvalue $\lambda_n(\beta)$ is interpolated locally as function of β by means of a quadratic polynomial. For a relative accuracy of 10^{-8}, typically 7 eigenvalue calculations were necessary in this iteration. An example of the iteration for the waveguide of dimensions 2 μm$\times$1 μm, with refractive index 1.1 and with wavelength in vacuo 1 μm, is shown in Table II. The mesh used was 10×5.

The convergence of the approximated values for the propagation constants for an increasing number of elements is shown in Table III for the first three modes. The results correspond to the rectangular waveguide of Fig. 7. The parameter N_2 is the number of mesh points along the shorter side of the rectangle, the number of mesh points N_1 along the longer side is $2N_2$. The results indicate quadratic convergence in the mesh size h.

One might expect the use of higher-order basis functions such as piecewise linear or quadratic basis functions to yield

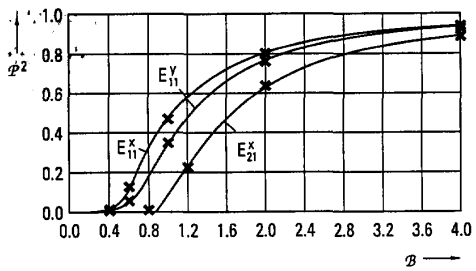

Fig. 8. Comparison of $\mathcal{P}^2$ as a function of $\mathcal{B}$ (see the text) of the smallest three modes of a rectangular waveguide of 2 μm × 1 μm, as computed by Goell and with the domain integral method. The mesh consists of 30 × 15 rectangles.

higher-order convergence. However, for waveguides with cross sections having corner points at which the normal derivative is discontinuous, the field is not smooth; therefore, using higher-order elements may not always yield better results.

In Fig. 8, computed propagation constants of the lowest three modes for a rectangular waveguide of 2 μm × 1 μm are compared to the results of Goell [8]. The mesh used in the computations consists of 30 × 15 elements. The symbols along the axis are defined by $\mathcal{P} = \{[(\beta/k)^2 - n_2^2]/[n_1^2 - n_2^2]\}^{1/2}$ and $\mathcal{B} = (dk/\pi)(n_1^2 - n_2^2)^{1/2}$, where k is the wavenumber in vacuo, d the shorter length of the guide, and n_1 and n_2 are the refractive indices of the guide and its exterior, respectively. The results agree well.

VI. Conclusions

The domain integral equation method, introduced by De Ruiter, Pichot, and Bagby *et al.* for the computation of guided modes in dielectric waveguides, is an accurate method for the vector theory. It applies to both inhomogeneous and anisotropic waveguides. A major advantage of the method is that, since the unknown field in the integral equation vanishes outside of the guide, only the guide itself has to be discretized.

In the domain integral equation, the propagation constant β of the guided modes occurs as a parameter in the kernel of a bounded symmetric integral operator. The computation of the propagation constants and fields of the guided modes amounts to determining β, such that one of the eigenvalues of the symmetric operator is equal to -1. These eigenvalues are characterized by the mini–max principles.

We use the Galerkin method to solve the eigenvalue problem for the domain integral operator instead of the more general method of moments, because the performance of the Galerkin method is much easier to analyze mathematically. As demonstrated in this paper, the application of the Galerkin method yields an algorithm that always converges when the mesh size is decreased. Hence, in particular, spurious solutions never occur. Furthermore, the Galerkin method enables the analysis of the order of convergence of the propagation constants and the approximative fields when the number of mesh points is increased.

Appendix

The integrals $I(v_1, v_2, m_1, m_2)$ (55) can be evaluated by the following procedure due to Boersma [4]. After rescaling, $I(v_1, v_2, m_1, m_2)$ becomes proportional to integrals of the form

$$\tilde{I}(v_1, v_2, m_1, m_2) = \frac{4}{\pi^2}\int_{-\infty}^{\infty}\int_{-\infty}^{\infty} \frac{\xi_1^{m_1-2}\xi_2^{m_2-2}}{\xi_1^2+\xi_2^2+1} \cdot \exp[i(a_1v_1\xi_1 + a_2v_2\xi_2)] \cdot \sin^2\left(\frac{a_1\xi_1}{2}\right)\sin^2\left(\frac{a_2\xi_2}{2}\right) d\xi_1\, d\xi_2 \quad (57)$$

for some $a_1, a_2 > 0$. The cases of interest are $m_1, m_2 = 0, 1, 2$ with $m_1 + m_2 \leq 2$. By expanding the sine factors in exponential functions, one finds

$$\begin{aligned}\tilde{I}(v_1, v_2) &= J(a_1(v_1-1), a_2(v_2-1)) \\ &\quad - 2J(a_1(v_1-1), a_2v_2) \\ &\quad + J(a_1(v_1-1), a_2(v_2+1)) \\ &\quad - 2J(a_1v_1\ \ , a_2(v_2-1)) \\ &\quad + 4J(a_1v_1\ \ , a_2v_2) \\ &\quad - 2J(a_1v_1\ \ , a_2(v_2+1)) \\ &\quad + J(a_1(v_1+1), a_2(v_2-1)) \\ &\quad - 2J(a_1(v_1+1), a_2v_2) \\ &\quad + J(a_1(v_1+1), a_2(v_2+1)) \end{aligned} \quad (58)$$

where

$$J(x, y) = \frac{1}{4\pi^2}\int_{-\infty}^{\infty}\int_{-\infty}^{\infty} \frac{\xi_1^{m_1-2}\xi_2^{m_2-2}}{\xi_1^2+\xi_2^2+1} \cdot \exp[i(x\xi_1 + y\xi_2)]\, d\xi_1\, d\xi_2. \quad (59)$$

The integrals are to be interpreted in the sense of Cauchy's principal value. Introducing m_1 and m_2 in the list of arguments of J, we get

$$\left.\begin{aligned} J(y, x, m_2, m_1) &= \ \ J(x, y, m_1, m_2) \\ J(-x, y, m_1, m_2) &= (-1)^{m_1}J(x, y, m_1, m_2) \\ J(x, -y, m_1, m_2) &= (-1)^{m_2}J(x, y, m_1, m_2) \end{aligned}\right\}. \quad (60)$$

For $x \geq 0$, $y \geq 0$, we have

$$J(x, y, 0, 2) = -\frac{1}{2\pi}\sqrt{x^2+y^2}K_1[\sqrt{x^2+y^2}] - \frac{x}{2\pi}\int_0^x K_0[\sqrt{t^2+y^2}]\, dt \quad (61)$$

$$J(x, y, 0, 0) = \frac{1}{4}xy + \frac{1}{\pi}\sqrt{x^2+y^2}K_1[\sqrt{x^2+y^2}] + \frac{x}{2\pi}\int_0^x K_0[\sqrt{t^2+y^2}]\, dt + \frac{y}{2\pi}\int_0^y K_0[\sqrt{x^2+t^2}]\, dt \quad (62)$$

$$-iJ(x, y, 0, 1) = -\frac{x}{4} + \frac{y}{2\pi} K_0[\sqrt{x^2+y^2}] + \frac{xy}{2\pi}\int_0^x \frac{K_1[\sqrt{t^2+y^2}]}{\sqrt{t^2+y^2}}\,dt - \frac{1}{2\pi}\int_0^y K_0[\sqrt{x^2+t^2}]\,dt. \quad (63)$$

$$J(x, y, 1, 1) = -\frac{1}{4} + \frac{y}{2\pi}\int_0^x \frac{K_1[\sqrt{t^2+y^2}]}{\sqrt{t^2+y^2}}\,dt + \frac{x}{2\pi}\int_0^y \frac{K_1[\sqrt{x^2+t^2}]}{\sqrt{x^2+t^2}}\,dt. \quad (64)$$

The integrals of the modified Bessel functions K_1 and K_0 on the right-hand side of (61)–(64) have to be computed numerically.

REFERENCES

[1] J. S. Bagby, D. N. Nyguist, and B. C. Drachman, "Integral formulation for analysis of integrated dielectric waveguides," *IEEE Trans. Microwave Theory Tech.*, MTT-33, pp. 906–915, Oct. 1985.

[2] N. H. G. Baken, M. B. J. Diemeer, J. M. van Slunter, and H. Blok, "Computational modeling of diffused channel waveguides using a domain integral equation," *J. Lightwave Technol.*, vol. 8, pp. 576–581, Apr. 1990.

[3] H. J. M. Bastiaansen, N. H. G. Baken, and H. Blok, "Domain-integral analysis of channel waveguides in anisotropic multi-layer media," *IEEE Trans. Microwave Theory Tech.*, vol. 40, pp. 1918–1926, Oct. 1992.

[4] J. Boersma, personal communication.

[5] P. G. Ciarlet, *The Finite Element Method for Elliptic Problems.* Amsterdam: North-Holland, 1979.

[6] R. Courant and D. Hilbert, *Methods of Mathematical Physics*, vol. II. New York: Wiley, 1962.

[7] R. Dautray and J.-L. Lions, "Integral equations and numerical methods," in *Mathematical Analysis and Numerical Methods for Science and Technology*, vol. 4. Berlin: Springer-Verlag, 1990.

[8] J. E. Goell, "A circular-harmonic computer analysis of rectangular dielectric waveguides," *Bell Syst. Tech. J.*, vol. 48, pp. 2133–2160, 1969.

[9] T. Kato, *Perturbation Theory for Linear Operators.* New York: Springer-Verlag, 1966.

[10] N. Mabaya, P. E. Lagasse, and P. Vanderbulcke, "Finite element analysis of optical waveguides," *IEEE Trans. Microwave Theory Tech.*, vol. MTT-29, pp. 600–605, 1981.

[11] M. Koshiba, K. Hayata, and M. Suzuki, "Finite-element method analysis of microwave and optical waveguides—Trends in countermeasures to spurious solutions," *Electron. Commun. Japan*, pt. 2, vol. 70, pp. 96–108, 1987.

[12] B. H. McDonald and A. Wexler, "Finite-element solution of unbounded field problems," *IEEE Trans. Microwave Theory Tech.*, vol. MTT-20, pp. 841–847, Dec. 1972.

[13] D. Marcuse, *Theory of Dielectric Optical Waveguides.* New York: Academic, 1974.

[14] M. J. McDougall and J. P. Webb, "Infinite elements for the analysis of open dielectric waveguides," *IEEE Trans. Microwave Theory Tech.*, vol. MTT-37, pp. 1724–1731, Nov. 1989.

[15] K. Hayata, M. Eguchi, and M. Koshiba, "Self-consistent finite/infinite element scheme for unbounded guided wave problems," *IEEE Trans. Microwave Theory Tech.*, vol. MTT-36, pp. 614–616, Mar. 1988.

[16] E. W. Kolk, N. H. G. Baken, and H. Blok, "Domain integral equation analysis of integrated optical channel and ridge waveguides in stratified media," *IEEE Trans. Microwave Theory Tech.*, vol. 38, pp. 87–85, 1990.

[17] Z. Pantic and R. Mittra, "Quasi-TEM analysis of microwave transmission lines by the finite-element method," *IEEE Trans. Microwave Theory Tech.*, vol. MTT-34, pp. 1096–1103, Nov. 1986.

[18] P. S. Pershan, "Magneto-optical effects," *J. Appl. Phys.*, vol. 38, pp. 1482–1490, 1967.

[19] C. Pichot, "Exact numerical solution for the diffused channel waveguide," *Opt. Commun.*, vol. 41, no. 3, pp. 169–173, Apr. 1982.

[20] B. M. A. Rahman, F. A. Fernandez, and J. B. Davies, "Review of finite element methods for microwave and optical waveguides," *Proc. IEEE*, vol. 79, pp. 1442–1448, Oct. 1991.

[21] B. M. A. Rahman and J. B. Davies, "Finite-element analysis of optical and microwave waveguides problems," *IEEE Trans. Microwave Theory Tech.*, vol. MTT-32, pp. 20–28, Jan. 1984.

[22] H. M. de Ruiter, "Integral-equation approach to the computation of modes in an optical waveguide," *J. Opt. Soc. Amer. A*, vol. 70, pp. 1519–1524, Dec. 1980.

[23] S. M. Saad, "Review of numerical methods for the analysis of arbitrarily shaped microwave and optical dielectric waveguides," *IEEE Trans. Microwave Theory Tech.*, vol. MTT-33, pp. 894–899, Oct. 1985.

[24] R. Sorrentino, "Review of numerical methods for passive components," in *1988 IEEE MTT-S Int. Microwave Symp. Dig.*, vol. 2, New York, May 1988, pp. 619–622.

[25] C.-C. Su, "A combined method for dielectric waveguides using the finite-element technique and the surface integral equations method," *IEEE Trans. Microwave Theory Tech.*, vol. MTT-34, pp. 1140–1146, Nov. 1986.

[26] H. P. Urbach, "Analysis of the domain integral operator for anisotropic dielectric waveguides," submitted to *SIAM J. Math. Anal.*

[27] K. Yoshida, *Functional Analysis.* Berlin: Springer-Verlag, 1980.

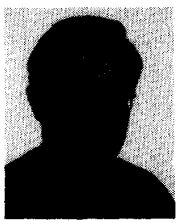

H. Paul Urbach received the M.S. degree in mathematics and the Ph.D. degree for a study of the optimization of hydrodynamic propulsion, from Groningen University, The Netherlands, in 1980 and 1985, respectively.

From 1980 until 1985, he was a Research Assistant in the Department of Mechanical Engineering and Mathematical Physics of Groningen University. Since 1986, he has been a member of the Applied Mathematics Group of Philips Research Laboratory in Eindhoven, The Netherlands, where his principal research subjects are electromagnetism and optics.

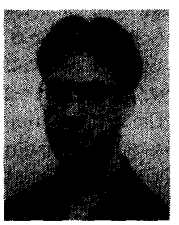

Eugène S. A. M. Lepelaars was born in Best, The Netherlands, in 1967. He received the M.S. degree in applied mathematics from the Eindhoven University of Technology in 1992.

During 1992, he was at Philips Research Laboratory in Eindhoven, The Netherlands, where he worked on the numerical modeling of dielectric waveguides. Since September 1992 he has been a Research Assistant in the Department of Electrical Engineering of Eindhoven University of Technology, where his doctoral program concerns the modeling of electromagnetic stimulation of human tissues.